

On the Properties of the Longitudinal RVB State in the Anisotropic Triangular Lattice. Mean-Field RVB Analytical Results.

A.L. Tchougréeff^{a,b} and R. Dronskowski^a

December 8, 2018

^aInstitut für anorganische Chemie RWTH-Aachen, Landoltweg 1, D-52056, Aachen, Germany;

^bPoncelet Lab., Independent University of Moscow, Moscow Center for Continuous Mathematical Education, Moscow, Russia.

Abstract

The spin-1/2 Heisenberg model on an anisotropic triangular lattice is considered in the mean-field RVB approximation. The analytical estimates for the critical temperatures of the longitudinal s-RVB state (the upper one) and the 2D s-RVB state (the lower one) are obtained which fairly agree with the results of the previous numerical studies on this system. Analytical formulae for the magnetic susceptibility and the magnetic contribution to the specific heat capacity in the longitudinal s-RVB state are obtained which fairly reproduce the results of the numerical experiment concerning these physical quantities.

1 Introduction

The RVB state originally proposed by Pauling [1] for describing the structure of benzene molecule as a superposition (resonance) of its Kekulé [2], Dewar [3], and Claus [4] structures as shown in Fig. 1 had been introduced into solid state physics by Anderson [5] in order to possibly explain the properties of

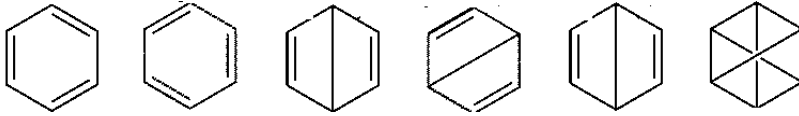


Figure 1: π -system of the benzene molecule. From left to right: two Kekulé resonance structures, three Dewar resonance structures, and the Claus resonance structure.

cuprate-based high-temperature superconductors. Since then this hypothetical ground state is being sought in many materials. Those exhibiting frustration of the exchange interactions of the magnetic momenta residing in them are widely suspected in forming a ground state of the RVB type. Among them the organic conductors of the family κ -(BEDT-TTF)₂Cu₂XY [6] and the halocuprates of the formula Cs₂CuCl₄ and Cs₂CuBr₄ [7] are considered as highly propable candidates. Recently CuNCN phase had been obtained and a series of measurements had been performed of its spatial structure and magnetic susceptibility, electric resistivity, heat capacity (all *vs. T*) [8]. Although on the basis of analogy with other materials of the MNCN series (M = Mn, Fe, Co, Ni) [9, 10, 11] one could expect more or less standard antiferromagnetic behavior, it turned out that in the low temperature phase the material at hand does not manifest any magnetic neutron scattering. The absence of the long range magnetic order (LRMO) (evanescence of the spin-spin correlation function) can be explained by the RVB character of the ground state of the system of the Cu²⁺ local spins 1/2 in this material. Close inspection of the materials structure (Fig. 2 from Ref. [8]) reveals that each Cu²⁺ ion can be effectively antiferromagnetically coupled to two its neighbors forming a chain while somewhat weaker antiferromagnetic coupling with four more neighbours from two adjacent parallel chains results in a Heisenberg model on an anisotropic triangular lattice with the Hamiltonian:

$$\sum_{\mathbf{r}} \sum_{\tau} J_{\tau} \mathbf{S}_{\mathbf{r}} \mathbf{S}_{\mathbf{r}+\tau} \quad (1)$$

where the coupling vectors τ take three values τ_i ; $i = 1 \div 3$; $\tau_1 = (1, 0)$; $\tau_2 = (\frac{1}{2}, \frac{\sqrt{3}}{2})$; $\tau_3 = (\frac{1}{2}, -\frac{\sqrt{3}}{2})$ with the interaction of the strength J along the lattice vector τ_1 (two neighbors) and with a somewhat smaller strength J' along the lattice vectors τ_2 and τ_3 (two neighbors along each). This is precisely the setting for which Hayashi and Ogata proposed that two (different) spin-singlet RVB (s-RVB) states are formed at different temperatures depending

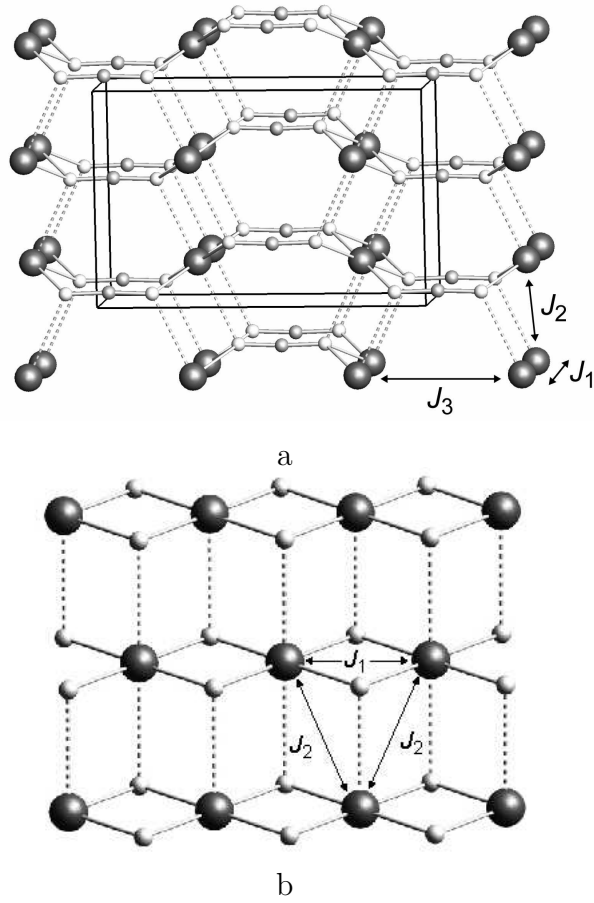


Figure 2: ab planes of the CuNCN crystal. A stronger J_1 extends in the a direction; somewhat weaker J_2 extends along the $b \pm a$ directions. The weakest J_3 extends in the c direction and is not considered in the present paper.

on the amount of anisotropy $\frac{J'}{J}$ resulting in a temperature dependence of the magnetic susceptibility with characteristic discontinuities corresponding to installment of these two respective states [12].

In the present paper we reasses their numerical results analytically partially with use of the Ginzburg-Landau phase transition theory in order to further apply the obtained analytical formulae to the experimental data obtained for CuNCN [8].

2 RVB mean-field analysis of anisotropic triangular lattice system

2.1 Equations of motion and self consistency equations

Hayashi and Ogata [12] base their analysis of the Hamiltonian eq. (1) on returning to the electron representation from the spin representation by the standard formulae:

$$\mathbf{S}_i = \frac{1}{2} c_{i\alpha}^+ \boldsymbol{\sigma}_{\alpha\beta} c_{i\beta}, \quad (2)$$

where $c_{i\sigma}^+$ ($c_{i\sigma}$) are the electron creation (annihilation) operators subject to the Fermi anticommutation relations; $\boldsymbol{\sigma}_{\alpha\beta}$ are the elements of the Pauli matrices and the summation over repeating indices is assumed. For the latter one can derive equations of motion based on the Heisenberg representation in which each operator obeys the following equation of motion:

$$i\hbar\dot{A} = [A, H] \quad (3)$$

where $[,]$ stands for the commutator of the operators and $\dot{}$ for the time derivative. Applying this to the creation and annihilation operators $c_{\mathbf{r}\sigma}^+$ ($c_{\mathbf{r}\sigma}$) and performing commutation, mean field decoupling and Fourier transformation as done in Appendix A results in mean field equations of motion for these operators :

$$\begin{aligned} i\hbar\dot{c}_{\mathbf{k}\sigma} &= -\frac{3}{2} \sum_{\tau} J_{\tau} \xi_{\tau} \cos(\mathbf{k}\tau) c_{\mathbf{k}\sigma} - \frac{3}{2} \sum_{\tau} J_{\tau} \Delta_{\tau} \cos(\mathbf{k}\tau) c_{-\mathbf{k}-\sigma}^+ \\ i\hbar\dot{c}_{\mathbf{k}\sigma}^+ &= \frac{3}{2} \sum_{\tau} J_{\tau} \xi_{\tau} \cos(\mathbf{k}\tau) c_{\mathbf{k}\sigma}^+ + \frac{3}{2} \sum_{\tau} J_{\tau} \Delta_{\tau}^* \cos(\mathbf{k}\tau) c_{-\mathbf{k}-\sigma} \end{aligned} \quad (4)$$

These latter reduces to the set of 2×2 eigenvalue problems for each wave vector \mathbf{k} :

$$\begin{pmatrix} \xi_{\mathbf{k}} & \Delta_{\mathbf{k}} \\ \Delta_{\mathbf{k}}^* & -\xi_{\mathbf{k}} \end{pmatrix} \begin{pmatrix} u_{\mathbf{k}} \\ v_{\mathbf{k}} \end{pmatrix} = E_{\mathbf{k}} \begin{pmatrix} u_{\mathbf{k}} \\ v_{\mathbf{k}} \end{pmatrix}$$

with

$$\begin{aligned} \xi_{\mathbf{k}} &= -3 \sum_{\tau} J_{\tau} \xi_{\tau} \cos(\mathbf{k}\tau) \\ \Delta_{\mathbf{k}} &= 3 \sum_{\tau} J_{\tau} \Delta_{\tau} \cos(\mathbf{k}\tau) \end{aligned} \quad (5)$$

(summation over τ extends to $\pm\tau_i; i = 1 \div 3$) which results in the eigenvalues (excitation spectrum) of the form:

$$E_{\mathbf{k}} = \sqrt{\xi_{\mathbf{k}}^2 + |\Delta_{\mathbf{k}}|^2} \quad (6)$$

whose eigenvectors are combinations of the destruction and creation operators with the above Bogoliubov transformation coefficients $u_{\mathbf{k}}, v_{\mathbf{k}}$. These equations result in the selfconsistency equations of the form:

$$\begin{aligned} \xi_{\tau} &= -\frac{1}{2N} \sum_{\mathbf{k}} \exp(i\mathbf{k}\tau) \frac{\xi_{\mathbf{k}}}{E_{\mathbf{k}}} \tanh\left(\frac{E_{\mathbf{k}}}{2\theta}\right) \\ \Delta_{\tau} &= \frac{1}{2N} \sum_{\mathbf{k}} \exp(-i\mathbf{k}\tau) \frac{\Delta_{\mathbf{k}}}{E_{\mathbf{k}}} \tanh\left(\frac{E_{\mathbf{k}}}{2\theta}\right) \end{aligned} \quad (7)$$

for six order parameters $\xi_{\tau}, \Delta_{\tau}$.

2.2 Free energy

Following Ref. [14] one can write immediately the free energy in terms of the above order parameters:

$$-\frac{\theta}{2N} \sum_{\mathbf{k}} \ln \left(2 \cosh \left(\frac{E_{\mathbf{k}}}{2\theta} \right) \right) + \frac{3}{2} \sum_{\tau} J_{\tau} \xi_{\tau}^2 + \frac{3}{2} \sum_{\tau} J_{\tau} |\Delta_{\tau}|^2 \quad (8)$$

(summation over τ extends to $\pm\tau_i; i = 1 \div 3$). Minima of this expression correspond to various possible states of the system. This is more informative than studying the self consistency equations eq. (7) which may have more solutions. *E.g.* the trivial solution

$$\xi_{\tau} = \Delta_{\tau} = 0$$

always exist although may be not of the lowest energy (see below).

3 Simplified model of s-RVB on the anisotropic triangular lattice

The numerical analysis of Ref. [12] shows that in agreement with general theorems Ref. [13] the order parameters satisfy additional phase relations (see Appendix A.3 for details) which allows to reduce the number of order parameters to only two:

$$\sqrt{2}\xi = \xi_{\tau_1}; \sqrt{2}\eta = |\Delta_{\tau_2}| = |\Delta_{\tau_3}|$$

the first responsible for establishing the s-RVB state within the chains (longitudinal s-RVB) and the second for the same in the transversal direction (2D s-RVB). For the triangular anisotropic lattice as represented in the above approximation one can easily write the explicit expression for the free energy as relying on the general expression eq. (8). It reads as follows:

$$F = 6J\xi^2 + 12J'\eta^2 - \frac{\theta\sqrt{3}}{4\pi^2} \int_{BZ} \ln \left(2 \cosh \left(\frac{E_{\mathbf{k}}}{2\theta} \right) \right) d^2\mathbf{k}, \quad (9)$$

where $\theta = k_B T$ and

$$E_{\mathbf{k}}^2 = 18 \left[J^2 \xi^2 \cos^2(\mathbf{k}_x) + J'^2 \eta^2 \left(\cos^2\left(\frac{\mathbf{k}_x}{2} + \frac{\mathbf{k}_y\sqrt{3}}{2}\right) + \cos^2\left(\frac{\mathbf{k}_x}{2} - \frac{\mathbf{k}_y\sqrt{3}}{2}\right) \right) \right]$$

It is easy to check that for $\theta \rightarrow 0$ the integral produces an expression which is uniform with respect to ξ and η so that the minimum of the free energy corresponds to both order parameters nonvanishing (see also below):

$$\xi(\theta \rightarrow 0) \neq 0; \eta(\theta \rightarrow 0) \neq 0.$$

At high temperature we can use a high-temperature expansion:

$$\ln \left(2 \cosh \left(\frac{E_{\mathbf{k}}}{2\theta} \right) \right) \approx \ln 2 + \frac{1}{2} \left(\frac{E_{\mathbf{k}}}{2\theta} \right)^2 - \frac{1}{12} \left(\frac{E_{\mathbf{k}}}{2\theta} \right)^4$$

which allows to be integrated explicitly. This results in the Ginzburg-Landau approximate free energy $F_{GL}(\xi, \eta, \theta)$ which is of the fourth power in ξ and η . The critical temperatures in this approximation correspond to those where the free energy F_{GL} of a state with one or two nonvanishing order parameters

becomes lower than that of some other state (*e.g.* of the paramagnetic state with vanishing order parameters). It happens at:

$$\theta_c = \frac{3}{8}J, \quad (11)$$

where the longitudinal s-RVB state with:

$$\xi = \frac{2\sqrt{2}\theta\sqrt{1-\theta/\theta_c}}{3J}; \eta = 0 \quad (12)$$

installs (in perfect correspondence to the analytical result announced in Ref. [12]) and at

$$\theta'_c = \frac{3JJ'}{8(3J-2J')} \quad (13)$$

with

$$\frac{\theta_c}{\theta'_c} = \frac{3J}{J'} - 2 > 1.$$

Below the lower critical temperature eq. (13) the 2D-RVB state installs with the order parameters:

$$\begin{aligned} \xi &= \frac{2\sqrt{2}\theta}{3J} \sqrt{\left(1 - \frac{\theta}{\theta_c}\right) - \frac{4}{7}\left(1 - \frac{\theta}{\theta'_c}\right)} \\ \eta &= \sqrt{\frac{8}{21}\frac{\theta}{J'}} \sqrt{1 - \frac{\theta}{\theta'_c}} \end{aligned} \quad (14)$$

which is in fair agreement with the numerical result of Ref. [12] in that sense that it shows some depletion of the longitudinal order parameter (ξ) below the critical temperature of the transition to the 2D-RVB state. The order parameters' estimates are obtained as solutions for the minimum conditions for the Landau-Ginzburg free energy $\partial F_{\text{GL}}(\xi, \eta, \theta)/\partial \xi = \partial F_{\text{GL}}(\xi, \eta, \theta)/\partial \eta = 0$ as functions of θ . The lower critical temperature eq. (13) is, as one can expect, an overestimate of the exact critical temperature usual for the mean field theory as combined with the high-temperature expansion. It is, nevertheless, in a reasonable agreement with the numerical results of Ref. [12] where θ'_c/θ_c was estimated to be 0.213 for $J'/J = 0.6$ whereas our estimate is 1/3 for this amount of anisotropy.

For the longitudinal s-RVB phase eq. (12) further analysis is possible. The integral term in the limit $\theta \rightarrow 0$ reduces to

$$-\frac{1}{\pi} \int_{-\frac{\pi}{2}}^{\frac{\pi}{2}} E_{\mathbf{k}} d\mathbf{k}_x = -\frac{6\sqrt{2}}{\pi} J\xi$$

with use of the integration method as described in Appendix C. As combined with the term squared in ξ in the free energy eq. (9) this yields the amplitude of the order parameter ξ reached at the zero temperature:

$$\xi_0 = \frac{1}{\sqrt{2\pi}}, \quad (15)$$

which is in perfect agreement with the numerical result of Ref. [12].

4 Physical properties of the anisotropic triangular Heisenberg model

Qualitatively the behavior of the anisotropic triangular Heisenberg model looks as follows: order parameters related to the intrachain and interchain interactions are both vanishing above the higher critical temperature θ_c . The excitation spectrum is gapless and there is no dispersion in either direction so that paramagnetic behavior is to be expected (see below). Below the first critical temperature (since $\frac{J'}{J} < 1$) $\eta = 0$ (longitudinal s-RVB state) the excitations have the energy spectrum:

$$E_{\mathbf{k}} = 3\sqrt{2} |J\xi \cos(\mathbf{k}_x)| \quad (16)$$

with no dispersion in the transversal direction although with the temperature dependent bandwidth. The excitations propagating with the wave vectors with the longitudinal components equal to $\pm\frac{\pi}{2}$ are gapless. Below the lower critical temperature one can expect that provided the ratio $\frac{J'}{J}$ is not too large the spectrum acquires a finite gap for whatever wave vector. Due to qualitative changes in the spectrum of the system occurring at the two critical temperatures one can expect that the physical quantities which are predominantly contributed by the excitations with low energies will be significantly different in different phases. In what follows we shall derive analytical formulae for the magnetic contribution to the specific heat capacity and the

magnetic susceptibility in the longitudinal s-RVB state (between two critical temperatures eqs. (11), (13)) where only the order parameter ξ is nonvanishing. In the temperature range of interest the properties are predetermined by the vicinity of the gapless excitations along the lines $\mathbf{k}_x = \pm \frac{\pi}{2}$ in the Brillouin zone. However, the detailed form the spectrum must be immaterial for obtaining some semiquantitative estimates provided the qualitative features of the spectrum are captured. This can be done with use of a saw-like model dispersion law:

$$E_{\mathbf{k}} = 3\sqrt{2} \left| J\xi \left(1 - \frac{2|\mathbf{k}_x|}{\pi} \right) \right|, \quad (17)$$

which has the same gap behavior and the same bandwidth as the exact problem. It corresponds to the constant density of quasiparticle states in variance with the exact spectrum which is characterized by accumulation of the density at the top of the quasiparticle band.

4.1 Specific heat capacity

The magnetic contribution to the specific heat derives using the standard definition:

$$C_m = -2k_B T \frac{\partial}{\partial T} \sum_{\mathbf{k}} [f(E_{\mathbf{k}}) \ln f(E_{\mathbf{k}}) + (1 - f(E_{\mathbf{k}})) \ln(1 - f(E_{\mathbf{k}}))],$$

where

$$f(E) = \left[\exp\left(\frac{E}{\theta}\right) + 1 \right]^{-1}$$

is the Fermi distribution function. The specific heat capacity apparently vanishes in the gapless state (above θ_c). Replacing the summation by integration over BZ as described in Appendix C it becomes one per individual spin. After taking derivative with respect to T it becomes:

$$C_m = k_B \frac{\sqrt{3}}{16\pi^2} \int_{BZ} \frac{E_{\mathbf{k}} (E_{\mathbf{k}} - T E'_{\mathbf{k}} \xi') \operatorname{sech}^2\left(\frac{E_{\mathbf{k}}}{2\theta}\right)}{\theta^2} d^2\mathbf{k}.$$

where $E'_{\mathbf{k}}$ stands for the derivative of $E_{\mathbf{k}}$ with respect to ξ and ξ' stands for derivative of ξ with respect to T .

4.1.1 Saw-like spectrum

For the saw-like spectrum in the area where the integration is to be performed the following

$$E_{\mathbf{k}}(E_{\mathbf{k}} - TE'_{\mathbf{k}}\xi') = 18J^2(1 - \frac{2\mathbf{k}_x}{\pi})^2\xi(\xi - T\xi'),$$

holds, so that

$$C_m = k_B \frac{y^2(1 - T(\ln y)')}{\pi\theta^2} \int_0^{\frac{\pi}{2}} (1 - \frac{2x}{\pi})^2 \text{sech}^2\left(\frac{y(1 - \frac{2x}{\pi})}{2\theta}\right) dx,$$

where $y = 2\sqrt{3}J\xi$. The integration can be performed explicitly, which yields:

$$\left(\frac{\tanh\left(\frac{y}{2\theta}\right)}{\theta} - \frac{1}{\theta} - \frac{4}{y} \ln\left(1 + e^{-\frac{y}{\theta}}\right) + \frac{\pi^2\theta}{3y^2} + \frac{4\theta\text{Li}_2\left(-e^{-\frac{y}{\theta}}\right)}{y^2} \right) y(1 - T(\ln y)') \quad (18)$$

For the divergent $\frac{y}{\theta}$ one can expand hyperbolic tangent, the logarithm, and polylogarithm, and make sure that the divergent terms cancel each other and that the dominant contribution to the specific heat capacity is linear in temperature:

$$C_m = \frac{\pi^2\theta}{3y} (1 - T(\ln y)') k_B = \frac{\pi^2\theta}{9\sqrt{2}J\xi} k_B$$

(correction to it is at best proportional to $\frac{y}{\theta}e^{-\frac{y}{\theta}}$ which clearly disappears for the divergent $\frac{y}{\theta}$). On the other end of the interval – at the critical temperature θ_c , by contrast, $\frac{\theta}{y}$ diverges according to the divergence law of ξ . Expanding the first bracket in the above expression eq. (18) at small values of ξ we obtain:

$$C_m = k_B \frac{3J^2\xi^2}{\theta^2} (1 - T(\ln \xi)'). \quad (19)$$

This exact result can be combined with the classical expression for the temperature dependence of the order parameter in the vicinity of the critical point (for the reasons which will be clear below we use here a generalized form of the classical temperature dependency of the order parameter $(1 - \theta/\theta_c)^{1/2}$ which shows the same critical exponent as the classical one):

$$\begin{aligned} \xi &= \xi_0 \sqrt{1 - (\theta/\theta_c)^\alpha} \\ T\xi' &= -\frac{\alpha}{2}\xi_0 \left(\frac{\theta}{\theta_c}\right)^\alpha \frac{1}{\sqrt{1 - (\theta/\theta_c)^\alpha}} \end{aligned} \quad (20)$$

First term in the brackets eq. (19) when multiplied by ξ^2 is small in a vicinity of θ_c . The second term yields:

$$-\frac{T\xi'}{\xi} = \frac{\alpha}{2} \left(\frac{\theta}{\theta_c}\right)^\alpha \frac{1}{1 - (\theta/\theta_c)^\alpha} = \frac{\alpha}{2} \left(\frac{\theta}{\theta_c}\right)^\alpha \left(\frac{\xi_0}{\xi}\right)^2$$

so that, combining this with eq. (19) we obtain the finite jump of the magnetic contribution to the specific heat capacity in the critical point:

$$\Delta C_m(\theta_c) = k_B \frac{3J^2\alpha}{\theta_c^2} \xi_0^2 = \frac{16\alpha}{3\pi^2} k_B. \quad (21)$$

This finite jump is qualitatively in agreement with general theory. Precise agreement with the numerical results of [12] is not achieved due to approximate form both of the spectrum and the temperature dependence of the order parameter used above. On the other hand required agreement can be achieved by fitting the value of α (see below).

4.1.2 Exact spectrum

If the exact spectrum is inserted in the general expression for the magnetic contribution to the specific heat capacity we get:

$$C_m = k_B \frac{y^2 (1 - T(\ln y)')}{\pi\theta^2} \int_0^{\frac{\pi}{2}} \cos^2 x \operatorname{sech}^2 \left(\frac{y \cos x}{2\theta} \right) dx,$$

We could not find analytical expression for this integral. However, the magnitude of the jump of the magnetic contribution to the specific heat capacity in the critical point can be estimated from an expansion of the above integral for small $y(\xi)$. The result in the vicinity of the critical point reads:

$$C_m = k_B \frac{9J^2\xi^2}{2\theta^2} (1 - T(\ln \xi)').$$

Combining this with the above expression for the logarithmic derivative of the order parameter we obtain:

$$\Delta C_m(\theta_c) = \frac{8\alpha}{\pi^2} k_B. \quad (22)$$

Analysis of the low temperature limit for the exact heat capacity will be performed elsewhere.

4.2 Magnetic susceptibility

We use the standard definition of the magnetic susceptibility per spin:

$$\chi = -2\mu_B^2 \frac{1}{N} \sum_{\mathbf{k}} \frac{\partial f(E_{\mathbf{k}})}{\partial E_{\mathbf{k}}}$$

The summation replaces by integration which yields:

$$\chi = -\frac{\mu_B^2 \sqrt{3}}{4\pi^2} \int_{BZ} \frac{\partial f(E_{\mathbf{k}})}{\partial E_{\mathbf{k}}} d^2\mathbf{k} \quad (23)$$

Following the recipe of Appendix B.1 we get for the susceptibility:

$$\chi = \frac{\mu_B^2 \sqrt{3}}{4\pi^2 \theta} \sum_{n=1}^{\infty} (-1)^{n+1} n \int_{BZ} \exp\left(-\frac{nE_{\mathbf{k}}}{\theta}\right) d^2\mathbf{k},$$

which is analyzed below.

4.2.1 High temperature ($\theta > \theta_c$) gapless state

In this state the argument of the function under integral equals to zero for all values of \mathbf{k} . Thus inserting $E_{\mathbf{k}} \equiv 0$ to the derivative of the Fermi distribution function

$$\frac{\partial f(E)}{\partial E} = -\frac{\exp(\frac{E}{\theta})}{\theta [\exp(\frac{E}{\theta}) + 1]^2} \quad (24)$$

we obtain:

$$\chi = \frac{\mu_B^2}{2\theta}; \theta > \theta_c$$

in perfect agreement with the numerical result reported by Hayashi and Ogata [12].

4.2.2 Longitudinal s-RVB state

In this state the gap is absent along the lines $\mathbf{k}_x = \pm \frac{\pi}{2}$ in the reciprocal space. Their vicinity provides major contribution to the susceptibility. It will be estimated below for the saw-like approximation of the spectrum and for the exact one.

Saw like approximation of the spectrum Performing the integration as described in Appendix C we get for the susceptibility:

$$\chi = \frac{\mu_B^2 \sqrt{2}}{J\xi} \frac{1}{3} \sum_{n=1}^{\infty} (-1)^{n+1} \left(1 - \exp\left(-\frac{3\sqrt{2}J\xi n}{\theta}\right) \right).$$

Summation of the constant term yields $\frac{1}{2}$ according to Appendix B.1 and the rest is just the geometric series so that the susceptibility becomes:

$$\chi = \frac{\mu_B^2 \sqrt{2}}{J\xi} \frac{1}{3} \left(\frac{1}{2} - \frac{\exp\left(-\frac{3\sqrt{2}J\xi}{\theta}\right)}{1 + \exp\left(-\frac{3\sqrt{2}J\xi}{\theta}\right)} \right),$$

which transforms into

$$\chi = \frac{\mu_B^2}{J\xi} \frac{1}{3\sqrt{2}} \tanh\left(\frac{3J\xi}{\sqrt{2}\theta}\right).$$

Qualitative behavior of the saw-spectrum model susceptibility The temperature behavior of the susceptibility in the saw approximation depends on that of $\xi(\theta)$. If the latter flows to a finite value while $\theta \rightarrow 0$ the susceptibility remains finite as well in agreement with finding of Ref. [12] for the longitudinal state. The limiting value equals $\frac{\pi}{3} \frac{\mu_B^2}{J}$ which is significantly higher than the numerical limiting value obtained in Ref. [12]. By contrast, if $\frac{\xi(\theta)}{\theta} \rightarrow \alpha > 0$ (the case of the temperature dependence provided by the high-temperature expansion eq. (12)), a paramagnetic behavior can be expected, although with the number of momenta effectively suppressed by hyperbolic tangens which is always less than unity.

Exact susceptibility in the longitudinal s-RVB state Using the integration trick as described in Appendix C and inserting the exact spectrum of the longitudinal state and noticing the argument of the absolute value is positive in the integration limits we obtain for the integral:

$$\begin{aligned} \int_{-\frac{\pi}{2}}^{\frac{\pi}{2}} \exp\left(-\frac{nE_{\mathbf{k}}}{\theta}\right) d\mathbf{k}_x &= \int_{-\frac{\pi}{2}}^{\frac{\pi}{2}} \exp\left(-\frac{n3\sqrt{2}J\xi \cos(\mathbf{k}_x)}{\theta}\right) d\mathbf{k}_x \\ &= \pi \left(I_0\left(\frac{n3\sqrt{2}J\xi}{\theta}\right) - L_0\left(\frac{n3\sqrt{2}J\xi}{\theta}\right) \right) \end{aligned}$$

where I_0 is the modified Bessel function and L_0 is the Struve function of the 0-th index. So that we arrive to the expression for the susceptibility in the longitudinal s-RVB state

$$\chi(\theta) = \frac{2\mu_B^2}{\theta} \sum_{n=1}^{\infty} (-1)^{n+1} n \left(I_0 \left(\frac{n3\sqrt{2}J\xi}{\theta} \right) - L_0 \left(\frac{n3\sqrt{2}J\xi}{\theta} \right) \right), \quad (25)$$

which is exact.

Qualitative behavior of the exact susceptibility The differences of the modified Bessel function and the Struve function in eq. (25) divided by θ have finite limit while $\theta \rightarrow 0$ which equals to

$$\frac{\sqrt{2}}{3\pi J\xi n}.$$

Inserting it into the series eq. (25) and performing summation according to Appendix B we obtain that at zero temperature the susceptibility in the longitudinal s-RVB state has finite limit

$$\chi = \frac{\mu_B^2 \sqrt{2}}{3\pi J\xi_0} = \frac{2\mu_B^2}{3J}$$

This is in perfect agreement with the numerical result of Ref. [12]. The ratio

$$\frac{\chi^{\text{exact}}(\theta = 0)}{\chi^{\text{saw}}(\theta = 0)} = \frac{2}{\pi} < 1$$

which is expectable due to accumulation of the quasiparticle states at the top of the exact spectrum *vs* uniform density of states for the saw-like spectrum. On the other hand in the vicinity of the critical temperature θ_c where order parameter is small in eq. (25) the series terms have finite limit of unity independently of the n value, which as combined with Appendix B.1 yields:

$$\chi(\theta_c) = \frac{\mu_B^2}{2\theta_c}$$

so that

$$\frac{\chi(\theta = 0)}{\chi(\theta_c)} = \frac{2\sqrt{2}\theta_c}{3\pi J\xi_0} = \frac{1}{2\sqrt{2}\pi\xi_0} < 1.$$

The susceptibility at the critical temperature θ_c is continuous as well in agreement with results of Ref. [12] as they are with the results of the saw-approximation for the spectrum.

High-temperature estimate for the temperature dependence of the susceptibility in the longitudinal s-RVB state At high temperatures (in the vicinity of the upper critical temperature) the temperature dependent bandwidths of the quasiparticle spectrum scaling the arguments of the functions in the series eq. (25) are small. Nevertheless the expansions of the modified Bessel function and the Struve function at small values of argument cannot be applied since the summation extends to arbitrary large values of n . For that reason in order to derive temperature dependence of the susceptibility in the vicinity of the upper critical point we apply the high-temperature expansion for the energy derivative of the Fermi distribution eq. (24) as described in Appendix B.2 and arrive to the formula:

$$\chi(\theta) = \frac{\mu_B^2}{2\theta} \left[1 + 4 \sum_{n=1}^{\infty} \left(\frac{y}{2\theta} \right)^n \frac{(2^{n+2} - 1) B_{n+2}}{\left(\frac{n!}{2!} \right)^2 (n+2)} \right], \quad (26)$$

to be used for numerical estimates.

Asymptotic estimate for the temperature dependence of the susceptibility in the longitudinal s-RVB state In order to elucidate the details of the temperature behavior of the susceptibility in the longitudinal s-RVB state close to the zero temperature (provided this state exist in this temperature region) and eventually valid above the lower critical value we performed analysis using asymptotic expansions for the Bessel and Struve functions at large values of their arguments (low temperatures) as described in Appendix B.3 and finally arrived to:

$$\chi = \frac{2\mu_B^2}{\pi y} \left(1 + \frac{1}{\sqrt{2\pi}} \sum_{k=1}^{\infty} \frac{\Gamma(\frac{1}{2} + k)}{\Gamma(k+1)} \left(\frac{\pi\theta}{y} \right)^{2k} (2^{2k} - 2) |B_{2k}| \right) \quad (27)$$

The performed analysis is valid provided the ratio $\frac{\xi(\theta)}{\theta}$ has nonvanishing limit or diverges while $\theta \rightarrow 0$. In this case the arguments of the Bessel function in eq. (25) remain large and the asymptotic expansion used in Appendix B.3 on which the final result is based remains valid.

4.2.3 Two-dimensional s-RVB state

In the region below the lower critical temperature θ'_c both order parameters ξ and η of the simplified model are nonvanishing and the spectrum has a

finite gap for all values of the wave vector in the BZ. Thus the susceptibility can be fairly approximated by a simple expression:

$$\chi = \frac{2\mu_B^2}{\theta} \frac{\exp(-\frac{\Delta}{\theta})}{[\exp(-\frac{\Delta}{\theta}) + 1]^2}$$

where Δ is some characteristic value of average gap (constant in the BZ) effectively taking into account both the gap and the dispersion of the quasiparticles. This expression describes exponentially decaying susceptibility provided $\frac{\Delta(\theta)}{\theta} \rightarrow \infty$ while $\theta \rightarrow 0$. This is in qualitative agreement with the numerical results of Ref. [12]. Further improvements can be expected from taking into account temperature dependence of the average gap below the lower critical temperature due to expected temperature dependence of the transversal and longitudinal order parameters.

5 Comparison with numerical experiment

It has been mentioned above that the precise temperature behavior of the physical quantities as coming from the analysis of the exact spectrum or with a saw-like model depend on the details of the temperature dependence of the order parameters ξ and η . The numerical results of Ref. [12] show that the both order parameters remain finite at $\theta = 0$. The high-temperature expansion as yielding the critical temperatures for the emergence of the both order parameters yields a linear evanescence of ξ in this limit in contradiction with results of numerical experiment and with the exact result eq. (15). Obviously the high-temperature expansion fails at low temperatures. On the other hand close inspection of the numerical results of Ref. [12, 16] shows that in addition to the vertical tangent characteristic to the $\xi(\theta)$ dependency at the upper critical temperature one has to count to visibly horizontal tangent at zero temperature. This indicates that the exponent α in eq. (20) must be larger than unity. With these precautions we shall establish relation between our analytical results and those of the numerical modeling in Ref. [12].

5.1 Heat capacity

According to calculations of Ref. [12] the magnetic contribution to the specific heat capacity experience a jump of $2k_B$ in the upper critical point.

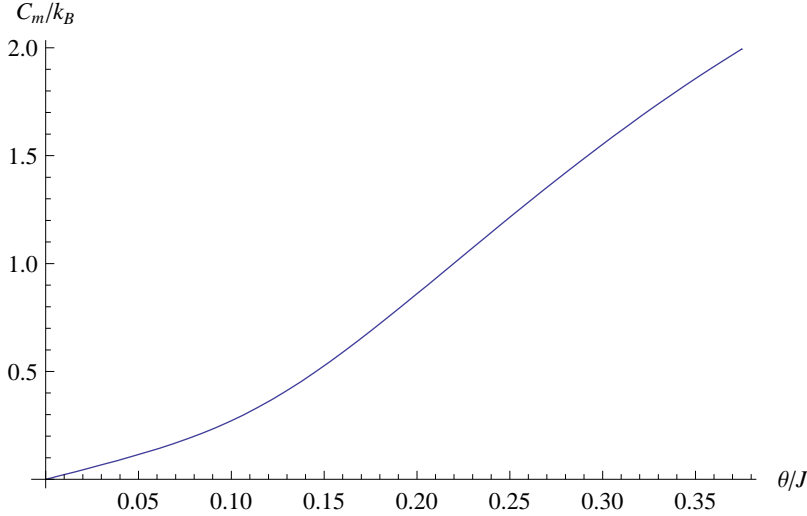


Figure 3: C_m vs θ as obtained by numerical integration with the exact spectrum and with generalized classical approximation for $\xi(\theta)$ ($\alpha = \pi^2/4$).

Combining this with our result eq. (22) we can derive $\alpha = \pi^2/4 \approx 2.46$. Corresponding graph represented in Fig. 3 shows perfect agreement with the numerical results of Ref. [12].

5.2 Magnetic susceptibility

The results of the model calculation on magnetic susceptibility per spin are represented in Fig. 4 for the generalized classical approximation for $\xi(\theta)$.

The temperature dependence of the susceptibility outside the longitudinal RVB region ($\theta < \theta'_c$, $\theta > \theta_c$) is given respectively by the average gap model and by paramagnetic susceptibility. Within the longitudinal RVB region ($\theta > \theta'_c$, $\theta < \theta_c$) the asymptotic expansion eq. (27) is used in the vicinity of the lower critical temperature and the high-temperature expansion eq. (26) in the vicinity of the upper critical point. The picture fairly shows the key features of the temperature dependence of the magnetic susceptibility of the longitudinal s-RVB state as they appear from the numerical calculation of Ref. [12]. The low-temperature limit is almost achieved pretty above the final exponential drop to zero characteristic for the low temperature 2D-RVB phase. The asymptotic and high-temperature expansions for the susceptibility of the longitudinal s-RVB state derived for low temperatures remain fairly

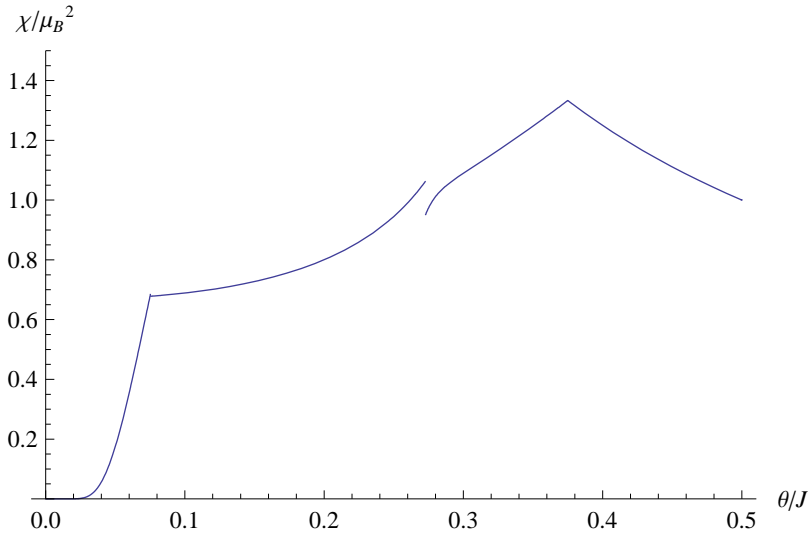


Figure 4: χ vs θ with generalized classical approximation for $\xi(T)$ ($\alpha = \pi^2/4$). and in . The susceptibility in the low-temperature phase (2D-RVB with both longitudinal and transversal order parameters nonvanishing) is drawn in the average gap approximation with the exact magnitude of the latter adjusted to assure continuous behavior of the susceptibility at the lower critical temperature. The interval of θ/J between θ'_c and $\frac{3}{11}J$ is drawn according to eq. (27) with $k_{max} = 1$. The interval of θ/J between $\frac{3}{11}J$ and θ_c is drawn according to eq. (26) up to 14-th power in reciprocal temperature.

valid (on respective sides) almost until quite arbitrary temperature $\frac{3}{11}J$ with the acceptable amount of discontinuity between two different expansions.

6 Conclusion

In the present paper we succeeded in obtaining analytical estimates for the critical temperatures of the installment of the longitudinal and 2D s-RVB states in the spin-1/2 Heisenberg model on the anisotropic triangular lattice in the Ginzburg-Landau approximation for arbitrary value of the anisotropy (in the assumption of the existence of the both longitudinal and 2D states). These estimates are in a fair agreement with the numerical results of Ref. [12] related to the same system, but apply for the arbitrary anisotropy value $\frac{J'}{J}$ in the allowed range. The method does not allow for obtaining correct estimates of the temperature dependence of the equilibrium values of the order parameters of the system. That of the longitudinal s-RVB state was interpolated with use of the generalized classical temperature dependence corresponding to the critical exponent 1/2 and scaled so that its value at zero temperature equals to that obtained by minimization of the zero temperature free energy.

For the longitudinal s-RVB state of the spin-1/2 Heisenberg model on the anisotropic triangular lattice, existing between the upper and lower critical temperatures the analytical estimate of the magnetic contribution to the specific heat capacity is obtained with use of the saw-like approximation for the quasiparticle spectrum. The low-temperature behavior of the magnetic contribution to the specific heat capacity coincides with that obtained numerically in Ref. [12]: it has a finite slope at $\theta \rightarrow 0$. On the other hand the magnitude of the abrupt jump of the magnetic specific heat capacity in the paramagnetic state (above the upper critical temperature) had been derived for the exact spectrum in agreement with general theory. In the generalized classical approximation of the temperature dependence of the order parameter its magnitude ($2k_B$) known from numerical experiment Ref. [12] can be reproduced under setting the α parameter of the generalized classical formula equal to $\pi^2/4$.

For the longitudinal s-RVB state of the spin-1/2 Heisenberg model on the anisotropic triangular lattice analytical expressions are obtained for the magnetic susceptibility for the saw-like model of the quasiparticle spectrum as well as for the exact spectrum. (In the latter case – the asymptotic estimates

have been obtained valid respectively in the vicinity of the lower and higher critical temperatures). Under assumption of the generalized classical temperature dependence of the longitudinal order parameter as the most realistic from the point of view of reproducing the results of numerical experiment on the magnetic contribution to the specific heat capacity the temperature dependence of the magnetic susceptibility in the longitudinal s-RVB state are fairly reproduced: the finite limit at the zero temperature (under condition of the existence of the longitudinal s-RVB state at this temperature) is obtained as well as the decrease of the susceptibility in the longitudinal phase as compared to the maximal value achieved at the upper critical temperature, separating the longitudinal s-RVB phase from the paramagnetic one. Narrow problematic region where both the low-temperature asymptotic and the high-temperature expansions are not good enough is found around $\theta \approx 3J/11$.

Acknowledgments

This work has been performed with the support of Deutsche Forschungsgemeinschaft and the Excellence Initiative of the German federal and state governments. In addition, we acknowledge the Russian Foundation for Basic Research for the financial support dispatched to ALT through the grant No. 10-03-00155. The authors are thankful to Prof. M. Ogata and Mr. Y. Hayashi for valuable discussion and valuable information which helped to improve the paper.

References

- [1] L. Pauling. The dynamic model of the chemical bond and its application to the structure of benzene. *J. Am. Chem. Soc.* 48, 1132 - 1143 (1926).
- [2] A. Kekulé (1865). "Sur la constitution des substances aromatiques". *Bulletin de la Societe Chimique de Paris* 3 (2): 98–110.
- [3] J. Dewar (1867). "On the Oxidation of Phenyl Alcohol, and a Mechanical Arrangement adapted to illustrate Structure in the Non-saturated Hydrocarbons". *Proc. Royal Soc. Edinburgh* 6,62: 96.

- [4] A. Claus, *Theoretische Betrachtungen und deren Anwendungen zur Systematik der organischen Chemie*, Freiburg, 1867, p. 207
- [5] Anderson, P.W. (1987). "The resonating valence bond state in La_2CuO_4 and superconductivity". *Science* 235 (4793): 1196–1198.
- [6] Y. Shimizu, K. Miyagawa, K. Kanoda, M. Maesato, and G. Saito, *Phys. Rev. Lett.* 91, 107001 (2003).
- [7] R. Coldea, D. A. Tennant, A. M. Tsvelik, and Z. Tylczynski, *Phys. Rev. Lett.* 86, 1335 2001; R. Coldea, D. A. Tennant, and Z. Tylczynski, *Phys. Rev. B* 68, 134424 2003; T. Ono, H. Tanaka, H. Aruga Katori, F. Ishikawa, H. Mitamura, and T. Goto, *Phys. Rev. B* 67, 104431 2003.
- [8] X.-H. Liu, R. Dronskowski, R.K. Kremer, M. Ahrens, C.-D. Lee, M.-H. Whangbo, *J. Phys. Chem. C* 112 (2008) 11013.
- [9] M. Krott, A. Houben, P. Müller, W. Schweika, and R. Dronskowski, *Phys. Rev. B* 80, 024117 (2009).
- [10] M. Krott, X. H. Liu, B. P. T. Fokwa, M. Speldrich, H. Lueken, and R. Dronskowski, *Inorg. Chem.* 46, 2204 (2007).
- [11] X. H. Liu, L. Strok, M. Speldrich, H. Lueken, and R. Dronskowski, *Chem. Eur. J.* 15, 1558 (2009).
- [12] Y. Hayashi and M. Ogata. *J. Phys. Conf. Ser.* 150 (2009) 042053.
- [13] M.Ogata, *J. Phys. Soc. Jpn.* 72 (2003) 1839; F.C.Zhang, C.Gros, T.M.Rice and H.Shiba, *Supercond. Sci. Technol.* 1 (1988) 36.
- [14] M. Ogata and H. Fukuyama. *Rep. Progr. Phys.* 71 (2008) 036501.
- [15] Y. Hayashi and M. Ogata. arXiv:0704.1313v1; Y.Hayashi and M.Ogata, *J. Phys. Soc. Jpn.* 76 (2007) 053705.
- [16] Y. Hayashi. Private communication.
- [17] *Handbook of Mathematical Functions*. M. Abramowitz, I.A. Stegun Eds. National Bureau of Standards Applied Mathematics Series # 55. (1964, 1972).

A Derivation of equations of motions

A.1 Equations of motion for Fermi operators

The equation of motion for the Fermi operators as coming from the Heisenberg spin Hamiltonian eq. (1) are based on the commutation relations between the Fermi operators and the spin operators as given by eq. (2). Inserting the explicit form of the tensor components of the spin operator:

$$\begin{aligned} S_i^+ &= c_{i\alpha}^+ c_{i\beta}; S_i^- = c_{i\beta}^+ c_{i\alpha}; \\ S_i^z &= (c_{i\alpha}^+ c_{i\alpha} - c_{i\beta}^+ c_{i\beta})/2 \end{aligned}$$

one obtains:

$$\begin{aligned} [c_{i\alpha}, \mathbf{S}_i \mathbf{S}_j] &= (c_{i\beta} S_j^- + c_{i\alpha} S_j^z)/2 \\ [c_{i\beta}, \mathbf{S}_i \mathbf{S}_j] &= (S_j^+ c_{i\alpha} - c_{i\beta} S_j^z)/2 \end{aligned}$$

with this we obtain in terms of the Fermi operators:

$$\begin{aligned} [c_{i\alpha}, \mathbf{S}_i \mathbf{S}_j] &= (c_{i\beta} c_{j\beta}^+ c_{j\alpha} + c_{i\alpha} (c_{j\alpha}^+ c_{j\alpha} - c_{j\beta}^+ c_{j\beta}))/2 \\ [c_{i\beta}, \mathbf{S}_i \mathbf{S}_j] &= (c_{j\alpha}^+ c_{j\beta} c_{i\alpha} - c_{i\beta} (c_{j\alpha}^+ c_{j\alpha} - c_{j\beta}^+ c_{j\beta}))/2 \end{aligned}$$

which must be inserted for each terms in eq. (1).

A.2 Mean field decoupling of equations of motion

The terms contributing to the right hand side of equations of motion for Fermi operators as derived in the previous Section are all of the third overall power with respect to these operators. If one is interested in having an option for superconducting (anomalous) state the mean-field decoupling has to read as:

$$c_1^+ c_2 c_3 \Rightarrow \langle c_1^+ c_2 \rangle c_3 - \langle c_1^+ c_3 \rangle c_2 + c_1^+ \langle c_2 c_3 \rangle$$

where the superconducting anomalous averages appear. In the RVB state we are going to take care of it is reasonable to set

$$\langle c_{j\alpha}^+ c_{j\alpha} \rangle = \langle c_{j\beta}^+ c_{j\beta} \rangle = \frac{1}{2}.$$

In order to assure the S_z conservation we set

$$\langle c_{i\alpha} c_{j\alpha} \rangle = \langle c_{i\beta} c_{j\beta} \rangle = 0$$

$$\langle c_{\sigma}^{+} c_{-\sigma} \rangle = 0$$

After further assuming the translational invariance and effectively introducing order parameters ξ_{τ} :

$$\begin{aligned} \langle c_{i\alpha}^{+} c_{j\alpha} \rangle &= \langle c_{i\beta}^{+} c_{j\beta} \rangle = \xi_{j-i} \\ \xi_{\tau} &= \langle c_{\mathbf{r}+\tau\sigma}^{+} c_{\mathbf{r}\sigma} \rangle \end{aligned}$$

$$\begin{aligned} \langle c_{j\alpha} c_{i\beta} \rangle &= \langle c_{i\alpha} c_{j\beta} \rangle = \Delta_{ij} = \Delta_{ji} \\ \langle c_{j\beta} c_{i\alpha} \rangle &= \langle c_{i\beta} c_{j\alpha} \rangle = -\Delta_{ij} = -\Delta_{ji} \end{aligned}$$

$$\begin{aligned} \langle c_{\mathbf{r}+\tau\alpha} c_{\mathbf{r}\beta} \rangle &= \langle c_{\mathbf{r}\alpha} c_{\mathbf{r}+\tau\beta} \rangle = \Delta_{\tau} = \Delta_{-\tau} \\ \langle c_{\mathbf{r}+\tau\beta} c_{\mathbf{r}\alpha} \rangle &= \langle c_{\mathbf{r}\beta} c_{\mathbf{r}+\tau\alpha} \rangle = -\Delta_{\tau} = -\Delta_{-\tau} \end{aligned}$$

Inserting these results in the equation of motion and using the Fourier transforms for the annihilation operators

$$c_{\mathbf{k}\sigma} = \frac{1}{\sqrt{N}} \sum_{\mathbf{r}} \exp(-i\mathbf{k}\mathbf{r}) c_{\mathbf{r}\sigma}$$

(N is the number of sites in the crystal) and hermitean conjugate one for the creation operators we arrive to:

the final equations of motion of the form:

$$\begin{aligned} i\hbar\dot{c}_{\mathbf{k}\alpha} &= -\frac{3}{2} \sum_{\tau} J_{\tau} \xi_{\tau} \cos(\mathbf{k}\tau) c_{\mathbf{k}\alpha} + \frac{3}{2} \sum_{\tau} J_{\tau} \Delta_{\tau} \cos(\mathbf{k}\tau) c_{-\mathbf{k}\beta}^{+} \\ i\hbar\dot{c}_{\mathbf{k}\beta} &= -\frac{3}{2} \sum_{\tau} J_{\tau} \xi_{\tau} \cos(\mathbf{k}\tau) c_{\mathbf{k}\beta} - \frac{3}{2} \sum_{\tau} J_{\tau} \Delta_{\tau} \cos(\mathbf{k}\tau) c_{-\mathbf{k}\alpha}^{+} \end{aligned}$$

where summation over τ is extended to $\pm\tau_i; i = 1 \div 3$.

A.3 Phase relations for order parameters

As it can be seen from the definitions eq. (5) of the dispersion functions and the requirement that the final form of the expression eq. (6) must be the square root of a sum of square terms referring to each τ as is *mutatu mutandis* eq. (12) of Ref.[15]:

$$E_{\mathbf{k}}^2 = 18 \left[J^2 \xi^2 \cos^2(\mathbf{k}_x) + J'^2 \eta^2 \left(\cos^2\left(\frac{\mathbf{k}_x}{2} + \frac{\mathbf{k}_y \sqrt{3}}{2}\right) + \cos^2\left(\frac{\mathbf{k}_x}{2} - \frac{\mathbf{k}_y \sqrt{3}}{2}\right) \right) \right],$$

where we set $\xi = \sqrt{2}D_1$ and $\eta = \sqrt{2}D_{23}$. It can be achieved if the cross terms between the contributions with from different τ 's cancel each other. This can be done by specific selection of the relative phases and amplitudes of the six order parameters ξ_τ and Δ_τ . We assume that

$$\Delta_\tau = \eta_\tau e^{i\varphi_\tau}.$$

Then the condition for disappearance of the cross terms in the expression for $E_{\mathbf{k}}^2$ reads:

$$\xi_\tau \xi_{\tau'} = -\eta_\tau \eta_{\tau'} \cos(\varphi_\tau - \varphi_{\tau'})$$

for all unordered pairs τ, τ' (three conditions). They can be nontrivially satisfied *e.g.* by the following choice (not unique due to SU(2) symmetry of the problem):

$$\begin{aligned} \eta_1 &= 0; \xi_1 \neq 0 \\ \eta_2 &\neq 0; \xi_2 = 0 \\ \eta_3 &\neq 0; \xi_3 = 0 \\ \frac{\pi}{2} &= \varphi_2 - \varphi_3 \\ \xi_1^2 &= 2\xi^2 \\ \eta_2^2 &= \eta_3^2 = 2\eta^2 \end{aligned}$$

which yields the required form of the excitation spectrum in the RVB phases.

B Series summation

In the present work we use asymptotic series as well as series not uniformly convergent. The sums of the latter are understood as limits of the functions they represent on the border of the convergency range. Examples follow.

B.1 Using geometric series for summation of divergent series

The Fermi distribution can be represented as a shifted geometric series:

$$\begin{aligned} \left[\exp\left(\frac{E}{\theta}\right) + 1 \right]^{-1} &= \frac{\exp\left(-\frac{E}{\theta}\right)}{1 + \exp\left(-\frac{E}{\theta}\right)} = \exp\left(-\frac{E}{\theta}\right) \sum_{n=0}^{\infty} (-1)^n \exp\left(-\frac{nE}{\theta}\right) \\ &= \sum_{n=0}^{\infty} (-1)^n \exp\left(-\frac{(n+1)E}{\theta}\right) \end{aligned}$$

which is the same as

$$\frac{x}{1+x} = x - x^2 + x^3 \dots = \sum_{n=0}^{\infty} (-1)^n x^{n+1}$$

with

$$x = \exp\left(-\frac{E}{\theta}\right)$$

This series converges for all $|x| < 1$ or $\theta > 0$, but at $x = 1$ it becomes a divergent series

$$\sum_{n=0}^{\infty} (-1)^n = 1 - 1 + 1 - 1 + 1 \dots$$

The function on the left hand, which defines the series, is continuous in $x = 1$ and the value of this function is taken as that of the sum of the divergent series:

$$\sum_{n=0}^{\infty} (-1)^n = \frac{1}{2}.$$

Analogous consideration applies to the derivative of the Fermi distribution with respect to the argument of the exponent:

$$-\frac{\exp(\frac{E}{\theta})}{[\exp(\frac{E}{\theta}) + 1]^2} = \sum_{n=0}^{\infty} (-1)^n (n+1) \exp\left(-\frac{(n+1)E}{\theta}\right).$$

Shifting the summation index by unity makes it a series:

$$\frac{x}{(1+x)^2} = -\sum_{n=0}^{\infty} (-1)^{n+1} (n+1) x^{n+1} = -\sum_{n=1}^{\infty} (-1)^n n x^n,$$

which is the derivative of the geometric series:

$$\frac{1}{1+x} = 1 - x + x^2 \dots = \sum_{n=0}^{\infty} (-1)^n x^n$$

$$\left(\frac{1}{1+x}\right)' = -\frac{1}{(1+x)^2} = \sum_{n=0}^{\infty} (-1)^n n x^{n-1} = \sum_{n=0}^{\infty} (-1)^{n+1} (n+1) x^n$$

multiplied by x . The series on the right hand side apparently diverges at $x = 1$ where it becomes:

$$-\sum_{n=1}^{\infty} (-1)^n n = -1 + 2 - 3 + 4 \dots$$

However, its sum, being defined as a limiting value of the function on left hand side, must be:

$$-\sum_{n=1}^{\infty} (-1)^n n = \frac{1}{4},$$

which is used throughout.

B.2 High-temperature expansion for the susceptibility in the longitudinal s-RVB state

In order to obtain the high-temperature expansion for the susceptibility we notice that the derivative of the Fermi distribution eq. (24) upto a numerical coefficient coincides with the generating function for the Euler polynomials $E_n(x)$ AS23.1.1¹:

$$\frac{\partial f}{\partial \varepsilon} = \sum_{n=0}^{\infty} \left(\frac{1}{\theta}\right)^{n+1} \frac{E_{n+1}(0)}{2n!} \varepsilon^n,$$

which is a good series expansion for small values of ε/θ (higher temperatures/small quasiparticle bandwidth). Inserting this and the exact quasiparticle spectrum $\varepsilon(\mathbf{k}_x)$ of the longitudinal s-RVB state in the definition of the magnetic susceptibility eq. (23) we obtain with account of the integration trick over the Brillouine zone in the longitudinal s-RVB state Appendix C for the susceptibility:

$$\chi = \frac{2\mu_B^2}{\pi} \sum_{n=0}^{\infty} \left(\frac{1}{\theta}\right)^{n+1} y^n \frac{E_{n+1}(0)}{2n!} \int_{-\frac{\pi}{2}}^{\frac{\pi}{2}} \cos^n x dx.$$

Inserting the values of integrals which are $\frac{\sqrt{\pi}\Gamma(\frac{n}{2}+\frac{1}{2})}{\Gamma(\frac{n}{2}+1)}$ and employing the equalities for the factorials and Gamma functions AS6.1.18 we arrive to:

$$\chi = \mu_B^2 \sum_{n=0}^{\infty} \left(\frac{1}{\theta}\right)^{n+1} \left(\frac{y}{2}\right)^n \frac{E_{n+1}(0)}{[(n/2)!]^2}.$$

¹Hereinafter ASnn.n.nn stands for the formula nn.n.nn of Ref. [17].

Then using AS23.1.20 we get

$$\chi = \frac{\mu_B^2}{2\theta} \left[1 + 4 \sum_{n=1}^{\infty} \left(\frac{y}{2\theta} \right)^n \frac{(2^{n+2} - 1)B_{n+2}}{[(n/2)!]^2 (n+2)} \right]$$

(here B_n are the Bernoulli numbers) to be used for numerical estimates.

B.3 Asymptotic low-temperature expansion of the susceptibility in the longitudinal s-RVB state

We make use of the asymptotic series AS12.2.6 for the difference of the Bessel and Struve functions:

$$I_0(x) - L_0(x) \sim \frac{1}{\pi} \sum_{k=0}^{\infty} \frac{(-1)^k \Gamma(\frac{1}{2} + k)}{\Gamma(\frac{1}{2} - k) \left(\frac{x}{2}\right)^{2k+1}}$$

valid for large values of argument:

$$x = \frac{n3\sqrt{2}J\xi}{\theta} = n\frac{y}{\theta}$$

i.e. for the lower temperatures. It is remarkable that the expansion behaves better for larger values of n . Inserting this expansion in the series for the susceptibility we get:

$$\chi = \frac{2\mu_B^2}{\pi\theta} \sum_{n=1}^{\infty} \sum_{k=0}^{\infty} (-1)^{n+1} n \frac{(-1)^k \Gamma(\frac{1}{2} + k)}{\Gamma(\frac{1}{2} - k) \left(\frac{ny}{2\theta}\right)^{2k+1}},$$

which results in:

$$\chi = \frac{2\mu_B^2}{\pi\theta} \sum_{n=1}^{\infty} \sum_{k=0}^{\infty} (-1)^{n+1} \frac{(-1)^k \Gamma(\frac{1}{2} + k)}{\Gamma(\frac{1}{2} - k) n^{2k}} \left(\frac{2\theta}{y}\right)^{2k+1}.$$

The summation over n then performs with use of AS23.2.19

$$\sum_{n=1}^{\infty} (-1)^{n+1} n^{-k} = (1 - 2^{1-k}) \zeta(k),$$

where $\zeta(k)$ is the Riemann zeta function, which results in:

$$\chi = \frac{2\mu_B^2}{\pi\theta} \sum_{k=0}^{\infty} \frac{(-1)^k \Gamma(\frac{1}{2} + k)}{\Gamma(\frac{1}{2} - k)} \left(\frac{2\theta}{y}\right)^{2k+1} (1 - 2^{1-2k}) \zeta(2k),$$

where the term with $k = 0$ yields:

$$\sum_{n=1}^{\infty} (-1)^{n+1} n \frac{2\theta}{ny} = \frac{\theta}{y},$$

according to Section B.1 so that:

$$\chi = \frac{2\mu_B^2}{\pi y} + \frac{2\mu_B^2}{\pi\theta} \sum_{k=1}^{\infty} \frac{(-1)^k \Gamma(\frac{1}{2} + k)}{\Gamma(\frac{1}{2} - k)} \left(\frac{2\theta}{y}\right)^{2k+1} (1 - 2^{1-2k}) \zeta(2k),$$

where the summation index k is shifted by unity. Next following AS23.2.16 we get

$$\chi = \frac{2\mu_B^2}{\pi y} + \frac{\mu_B^2}{\pi\theta} \sum_{k=1}^{\infty} \frac{(-1)^k \Gamma(\frac{1}{2} + k) (2\pi)^{2k}}{(2k)! \Gamma(\frac{1}{2} - k)} \left(\frac{2\theta}{y}\right)^{2k+1} (1 - 2^{1-2k}) |B_{2k}|,$$

where B_{2k} is the corresponding Bernoulli number.

Further simplification is performed with use of the formulae for the Gamma function. Using AS6.1.17:

$$\Gamma(z)\Gamma(1-z) = \frac{\pi}{\sin(\pi z)}$$

for $z = \frac{1}{2} + k$ we obtain

$$\begin{aligned} \Gamma\left(\frac{1}{2} - k\right) &= \frac{\pi}{\Gamma\left(\frac{1}{2} + k\right) \sin\left(\pi\left(\frac{1}{2} + k\right)\right)}; \\ \frac{1}{\Gamma\left(\frac{1}{2} - k\right)} &= \frac{(-1)^k \Gamma\left(\frac{1}{2} + k\right)}{\pi} \end{aligned}$$

so that

$$\chi = \frac{2\mu_B^2}{\pi y} + \frac{\mu_B^2}{\pi^2\theta} \sum_{k=1}^{\infty} \frac{\Gamma^2\left(\frac{1}{2} + k\right) (2\pi)^{2k}}{(2k)!} \left(\frac{2\theta}{y}\right)^{2k+1} (1 - 2^{1-2k}) |B_{2k}|$$

Inserting the definition of factorial in terms of Gamma function: $(2k)! = \Gamma(2k + 1)$ and applying the duplication formula AS6.1.18

$$(2k)! = \frac{1}{\sqrt{2\pi}} 2^{2k+1} \Gamma\left(\frac{1}{2} + k\right) \Gamma(k + 1),$$

we get:

$$\chi = \frac{2\mu_B^2}{\pi y} \left(1 + \frac{1}{\sqrt{2\pi}} \sum_{k=1}^{\infty} \frac{\Gamma(\frac{1}{2} + k)}{\Gamma(k + 1)} \left(\frac{\pi\theta}{y} \right)^{2k} (2^{2k} - 2) |B_{2k}| \right),$$

to be used for numerical estimates.

C Integration in the Brillouin zone of the trigonal lattice

The Brillouin zone (BZ) for the triangular lattice is a symmetric hexagon with a side $4\pi/3$ with the diagonal parallel to the \mathbf{k}_x axis in the reciprocal space. Its area equals to $8\pi^2/\sqrt{3}$ as employed in the expressions throughout the paper. The integration over BZ falls into three parts:

- one (1) over the bulk of the BZ: $\int_{-\frac{\pi}{2}}^{\frac{\pi}{2}} d\mathbf{k}_x \int_{-\frac{2\pi}{\sqrt{3}}}^{\frac{2\pi}{\sqrt{3}}} d\mathbf{k}_y$
- one (2) over stripes $2 \times \int_{\frac{\pi}{2}}^{\frac{2\pi}{3}} d\mathbf{k}_x \int_{-\frac{2\pi}{\sqrt{3}}}^{\frac{2\pi}{\sqrt{3}}} d\mathbf{k}_y$
- one (3) over triangles $4 \times \int_{\frac{2\pi}{3}}^{\frac{4\pi}{3}} d\mathbf{k}_x \int_0^{\frac{2\pi}{\sqrt{3}}} d\mathbf{k}_y$

We notice, however, that in the longitudinal s-RVB state the excitation spectrum is an even function of \mathbf{k}_x which consists of two branches each symmetric with respect to reflection in the straight lines $\mathbf{k}_x = \pm\pi$ which correspond to the ridges of the respective branches of the excitation spectrum. For that reason while integrating any function independent on \mathbf{k}_y over \mathbf{k}_y over the flaps of the BZ (the values of $\frac{2\pi}{3} \leq |\mathbf{k}_x| \leq \frac{4\pi}{3}$ – triangles integration) we see that for each given constant value of the integrand the length of the integration range corresponding to this value on one side of the ridge as summed with that on the other side of the ridge yields precisely $\frac{4\pi}{\sqrt{3}}$ which is the width of the BZ in the \mathbf{k}_y direction. For that reason the integration over \mathbf{k}_y in the flaps of the BZ is equivalent to integration over the rectangle $\frac{2\pi}{3} \leq \mathbf{k}_x \leq \pi; |\mathbf{k}_y| \leq \frac{2\pi}{\sqrt{3}}$, which after completing it with the integration over the rectangle $\frac{\pi}{2} \leq \mathbf{k}_x \leq \frac{2\pi}{3}; |\mathbf{k}_y| \leq \frac{2\pi}{\sqrt{3}}$ (stripe integration) becomes equal to

the integration over the bulk of the BZ, Thus the integral over the entire BZ in the longitudinal RBV state satisfies the condition:

$$\frac{\sqrt{3}}{8\pi^2} \int_{BZ} f(E_{\mathbf{k}}) d^2\mathbf{k} = \frac{1}{\pi} \int_{-\frac{\pi}{2}}^{\frac{\pi}{2}} f(E_{\mathbf{k}}) d\mathbf{k}_x$$

as used in our calculations.